MOLECULAR COUNTING OF LOW-DENSITY LIPOPROTEIN PARTICLES AS INDIVIDUALS AND SMALL CLUSTERS ON CELL SURFACES

DAVID GROSS AND WATT W. WEBB
School of Applied and Engineering Physics, Cornell University, Ithaca, New York 14853

ABSTRACT We employ the intensely fluorescent analogue diI-LDL (Barak, L. S., and W. W. Webb, 1981, *J. Cell Biol.* 90:595–604) as a counting marker to determine the numbers of LDL-receptor complexes that are contained in clusters on the surfaces of human fibroblasts and human epidermoid carcinoma cells. The application of quantitative digital intensified video optical microscopy allows the measurement of the fluorescence power collected from individual fluorescent spots on a cell with sufficient accuracy that the number of optically unresolved particles producing the fluorescence in the spot can be estimated. We demonstrate that isolated individual diI-LDL particles are detected on the surface of all cells investigated. Analysis of the LDL cluster size distributions on the various cell lines shows clear differences that correlate with efficiency of LDL metabolism. We find that normal fibroblasts (GM3348) have LDL-receptor complex populations dominated by large cluster sizes (>4 LDL), while internalization-deficient J.D. mutant fibroblasts (GM2408A) and epidermoid carcinoma cells (A-431) show predominantly small clusters (1-3 LDL). No evidence for large-scale ordering or "superclustering" of clusters is found.

INTRODUCTION

The dynamics and biochemistry of responses of living cells to receptor-specific ligands are of current general interest in a broad spectrum of biological problems (1, 2). Often the processing of a specific ligand proceeds through endocytosis at a specialized cell surface organelle, the coated pit, although other mechanisms of endocytosis are known. Processing via the coated pit pathway is commonly called receptor-mediated endocytosis. Most receptor-specific ligands, e.g., insulin, epidermal growth factor, and α-2-macroglobulin, bind to receptors that are initially randomly dispersed on the cell surface, but that cluster into coated pits upon ligand binding (3, 4). However, the normal receptor for the cholesterol-carrying plasma protein low density lipoprotein (LDL) appears to precluster on normal cells in coated pits before ligand challenge (5, 6). The amino acid sequence of the LDL receptor (LDL-R) has recently been elucidated (7–9); it is known that a 50-amino-acid residue on the carboxyl end of the LDL-R resides in the cytoplasm in vivo, and is responsible for the binding of the receptor to coated pits.

The work of Goldstein and Brown characterizes several mutant human fibroblast lines, including the J.D. or GM2408A, which do not internalize LDL by the normal coated pit mediated pathway (10, 11). They have found that the J.D. lesion is a single-point mutation in the cytoplasmic portion of the LDL-R, which is thought to inhibit the association of the receptor with clathrin coated pits on the cell surface without reducing the high affinity of the LDL-R for LDL (6). Recent measurements have shown that the diffusion coefficient of the liganded LDL-R complex (LDL-RC), although small, is large enough that the LDL-RC on J.D. cells can encounter coated pits on the cell surface at a rate sufficient to account for the observed internalization kinetics (12). This result supports the hypothesis that the defective coated pit binding of the LDL-R on J.D. cells is responsible for the inefficient internalization of LDL by these cells.

A second cell line, the human epidermoid carcinoma A-431, also expresses a mutated LDL-R that appears to interfere with the normal internalization of LDL (13). In contrast to J.D. cells, the A-431 LDL-RC cluster in large patches on cell surface extensions that protrude several nanometers out from the average plane of the plasma membrane, as judged by electron microscopy as well as in smaller clusters in coated pits (13). However, as with J.D. cells, the proportion of LDL-Rs in coated pits is much lower than that for normal fibroblasts.

To date, the quantitative estimation of the clustering of the LDL-RC has been accomplished by electron microscopy using electron-dense stains coupled to LDL to provide contrast. As cells must be fixed and embedded for observation in the electron microscope for this method of measurement, no dynamic morphological changes in the topography of receptor and ligand distribution can be measured on

Please address correspondence to Prof. Watt W. Webb, School of Applied and Engineering Physics, Clark Hall, Cornell University, Ithaca, New York 14853-2501

the single cell level. We describe here a new method based on optical microscopy that does not require cell fixation, and thus can easily be applied to study receptor-ligand dynamics.

EXPERIMENTAL METHODS

Digital Video Microscopy

All measurements described below were carried out on a Zeiss Universal Microscope (Carl Zeiss, Inc., Thornwood, NY) equipped with phase contrast optics, mercury arc epi-illumination for fluorescence excitation and a 100X 1.25 N.A. phase contrast objective. The microscope is interfaced to a Venus image intensifier vidicon camera (model TV2M; Venus Scientific, Inc., Farmingdale, NY). The video output of the camera is fed into the digitizing input of a Grinnell image processing system (model 274; Grinnell Systems, San Jose, CA), which is under interactive control of a PDP 11/23 computer (Digital Equipment Corp., Maynard, MA). Digitized video images are stored in real time in the three 512 × 480 × 8 bit volatile memory planes of the image processing system and are stored by computer data transfer on an 80 Mbyte Winchester hard disk (Model 5380; Kennedy Co., Monrovia, CA).

The video signal from the camera is digitized to 6-bits resolution by the image processing system. The digitized image is routed through video lookup tables, a 16-bit arithmetic and logic unit, a zoom and pan subsystem, and through a digital to analogue converter, which generates RGB video signals that drive a high resolution color monitor (Model C-3910; Mitsubishi Electric Co., Tokyo, Japan). All signal routing is under interactive computer control. Digital images stored in any of the three memory planes can be rapidly analyzed by image processing hardware for the grey level intensity content of a full frame, the maximum and minimum grey levels in a frame, and for the grey level values in any of the 245,760 pixels in the frame. Specialized interactive software has been developed to measure the intensity content and spatial distribution of the digital images contained in the memory planes. In particular, software to aid in the collection of the fluorescence power from a large number of fluorescent spots in an image was developed. The software allows the user to store a local background intensity that is subtracted from the integrated intensity of a bright spot, also selected by the user. Any spatial variation in camera gain and/or illumination intensity was corrected in the cell image by a procedure described elsewhere (14).

Cell Manipulations

GM3348 (normal) and GM2408A (J.D. internalization deficient) human fibroblast cell lines were obtained from the Human Genetic Mutant Cell Repository (Institute for Medical Research, Camden, NJ), while the A-431 epidermoid carcinoma cell line was a gift of Professor Efraim Racker (Section of Biochemistry, Wing Hall, Cornell University, Ithaca, NY). The fibroblast lines were grown in Dulbecco's Modified Eagle's Medium (DMEM) (Gibco, Grand Island, NY) supplemented with 10% vol/vol fetal calf serum (FCS) (Gibco). The carcinoma line was grown in DMEM supplemented with 10% calf serum (Gibco). Cell lines were cultured in 75 cm^2 flasks (Corning Medical, Corning Glass Works, Corning, NY) at 37°C in a humidified 5% CO_2 atmosphere incubator (National Appliance Company, Hollywood, FL). For experiments, cells were plated onto 22 × 22 mm No. 1 glass coverslips, 4 per 100 mm^2 plastic petri dish (Corning). After the cells had attached to the coverslips for 24–48 h, the number of LDL receptors expressed on the cell surfaces was upregulated by the method described by Brown et al. (15). In brief, cells were washed once with Medium 199 (M199) (Gibco), and 10 ml of DMEM plus 10% vol/vol delipidated FCS was added per dish. Cells were allowed to incubate for an additional 36–72 h in this medium.

LDL purification, reconstitution with diI(3), and tests of binding specificity were done according to the procedures of Barak and Webb (16). Live cell labeling was done at 4°C with all solutions prechilled to that temperature. Cells were prepared for labeling with diI-LDL by washing individual (Gibco) buffered to pH 7.3. DiI-LDL was diluted from stock solution into coverslips three times in M199 supplemented with 10 mM HEPES supplemented M199 to 12 μg/ml concentration and was applied prechilled at 4°C to the coverslips. The cells were incubated in the presence of diI-LDL for 15 min at 4°C, washed three times in cold phosphate buffered saline (PBS) (Gibco), and incubated for an additional 10–20 min in Hank's balanced salt solution (HBSS) (Gibco) supplemented with 2 mg/ml bovine serum albumin (Sigma Chemical Co., St. Louis, MO), 2 mM $CaCl_2$ and 10 mM TRIS at pH 7.3. Cells were then washed once in PBS and were fixed in PBS containing 3.7% formaldehyde for 5 min. For some experiments, GM3348 cells were stained with diI-LDL at 22°C for 15 min before competition with Hank's/BSA at 4°C and fixation with 3.7% formaldehyde. Coverslips were washed two times in PBS before mounting on a glass slide for observation.

Fluorescence Power Measurement

Each slide containing labeled cells was observed in both phase contrast and fluorescence by eye and with the video system. As the incident excitation light could be reduced dramatically when the intensified video camera was employed, all cells selected for analysis were observed only with the camera. A cell was prefocused in phase contrast illumination and then was epi-illuminated for fluorescence for ~1 s before a single video frame was stored in one of the memory planes. As the photobleaching decay time for diI-LDL at the illumination levels employed was of the order of minutes; no appreciable decay of the detected fluorescence occurred. Only those images for which a large number of diI-LDL fluorescent spots were in focus were stored for later analysis.

The fluorescence power collected from each diI-LDL spot is proportional to the spatial integral of the intensity forming the image of the spot minus the integral of the average local background intensity in the same region. As the background at the precise spot of bright fluorescence was not measurable, in practice the background collected from a neighboring area was taken as local background. Only those fluorescent spots that showed no resolvable structure were analyzed in this way. A small proportion of spots was clearly asymmetric, i.e., LDL particles were located at separations just resolvable by the optical microscope.

It is known that each diI-LDL particle contains on the average ~40 diI fluorophores (16). As an LDL particle is composed of a core of cholesterol ester surrounded by a monolayer coat of phospholipid, predominantly phosphatidylcholine, and a single species of apo-B protein embedded in the phospholipid, it is assumed that the fluorescent diI molecules incorporate into the outer phospholipid coat of the LDL. If the chromophore insertion is a random process, the fluorescence power distribution from a large collection of individual diI-LDL particles would be in the form of a Poisson distribution with mean number of particles equal to ~40. Since the expected relaxation times for translational and rotational diffusion of the chromophore are far smaller than the measurement time, the fluorescence power measurement averages over the entire population. If the mean number of diI fluorophores per LDL is n, then the fluorescence power distribution is

$$P_1(i) = \frac{n^i}{i!} e^{-n}, \tag{1}$$

where $P_1(i)$ is the single particle probability that i fluorophores (or i units of fluorescence power) are present in a given particle. If j LDL particles are clustered into a given spot of fluorescence, the corresponding fluorescence power probability distribution for the cluster is

$$P_j(i) = \sum_{k=0}^{i} P_{j-1}(k)\, P_1(i-k) = \frac{(jn)^i}{i!} e^{-jn}. \tag{2}$$

The probability distribution $P_j(i)$ derived from the single particle distribution in Eq. 1 by multiple iterations is mathematically equivalent to a Poisson distribution with a mean value of (jn). If there are N_j spots containing j unresolved diI-LDL particles, then the probability distribu-

tion for the whole population of spots is

$$P_T(i) = \frac{1}{N_T} \sum_{j=1}^{\infty} N_j P_j(i), \quad (3)$$

where

$$N_T = \sum_{j=1}^{\infty} N_j$$

is the total number of spots in the distribution.

An interactive computer program was developed to collect and analyze the fluorescence power distribution of the in-focus spots of diI-LDL in an image of an individual cell. The program integrates the total intensity in a user-selected region of the image, namely, a bright spot, and subtracts the integral of the average background of a nearby area that was also selected by the user as a region containing typical local background. Once the data are collected, they are binned into a histogram and the theoretical Poisson distribution of Eq. 3 is calculated and fit to the data by a numerical least-squares analysis. The fitting procedure is interactive in that the user has control over the values of the free parameters, namely, the mean number n of diI fluorophores per diI-LDL particle, the fluorescence power of an individual diI fluorophore, and the number of diI-LDL particles in the various cluster sizes from 1 to 20.

RESULTS

To test the hypothesis that the fluorescence power distribution from a population of diI-LDL particles bound to a cell can be described by Eq. 3, we measured the fluorescence power distribution for three normal human fibroblasts, one J.D. mutant fibroblast, and one A-431 carcinoma cell as described above. For each cell, ~50–200 spots of fluorescence were quantitated and analyzed.

Due to the relatively small number of low fluorescence power spots surveyed for an individual cell (~20–50), all the data for all cells were collected together and analyzed to best determine the first two of the free variables, namely, the mean number of fluorophores per diI-LDL and the fluorescence power of a single diI. The combined data from the five cells are shown in Fig. 1. It is clear from the figure that three peaks are present in the distribution and that the mean fluorescence powers of the peaks are integral multiples of a unit value, ~410 arbitrary fluorescence units. Least-squares analysis best fits a distribution with mean number of fluorophores per diI-LDL monomer of ~35 ± 3, and a mean peak fluorescence power of 411 ± 5. The best-fit theoretical multiple Poisson distribution of Eq. 3 is shown as a heavy line. The inset shows for comparison the theoretical distributions for different values of n, the mean number of fluorophores per monomer, to illustrate the effect of this parameter on the shape of the theoretical probability distribution.

The best-fit value for the mean number n of fluorophores per monomer is a lower limit to the true value since the spread of the fluorescence power data, which is the dominant factor in the determination of n, could also be affected by measurement uncertainty. To estimate this effect, 20 separate measurements of the fluorescence power of three different diI-LDL spots on a GM3348 fibroblast were made. For each measurement both the background area and the spot integration area were selected anew. The dominant source of uncertainty in measured fluorescence power was due to background subtraction. To estimate its maximum variation, background intensities were measured at random around the fluorescence spot. We found that the average maximum relative standard deviation in measured fluorescence power was 11%. Thus experimental uncertainty introduces an underestimate of the measured value of the mean number of fluorophores per diI-LDL particle of ~10% so that the best estimate is $n = 39$, in good agreement with the published value of 40 (16) for a different production lot of diI-LDL.

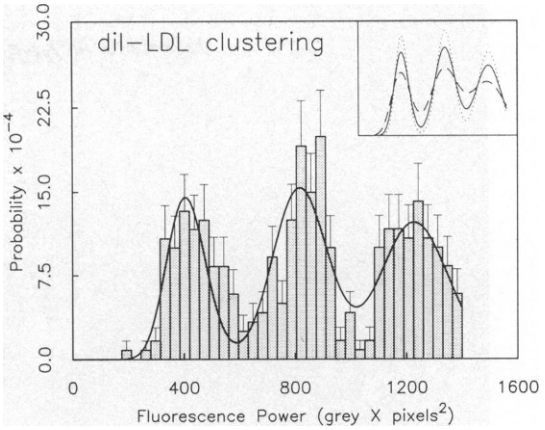

FIGURE 1 The measured fluorescence power distribution of small-size clusters of diI-LDL on three normal fibroblasts, one J.D. fibroblast, and one A-431 carcinoma cell. The low fluorescence power data were binned together to accumulate sufficient counts per fluorescence power bin to accurately measure the mean number of diI fluorophores per LDL as well as the mean fluorescence power of a single diI-LDL particle. The best-fit curve shown by the heavy solid line is for 35 diI molecules per diI-LDL particle of 411 arbitrary fluorescence power units. The *inset* shows the effect of varying the mean number of diI particles per diI-LDL; the *dotted line* is for $n = 50$, *solid line* is $n = 35$, and *dashed line* is $n = 20$. Larger values of n provide better separation of the peaks of the various cluster sizes.

The fluorescence images of four cells stained with diI-LDL are shown in Fig. 2. All four frames are the raw digital video images as displayed on and photographed from the video monitor. The upper left frame is an A-431 cell focused on its lamellipodium extending around the main cell body, which is mostly out of focus. The upper right frame is a GM2408A mutant fibroblast, focused predominantly near the center of the cell. The bottom two frames are of GM3348 normal fibroblasts; that on the left was stained at 4°C for 15 min, while that on the right was stained at 22°C for 15 min. The fluorescence power distributions for measured fluorescence spots on the cells of Fig. 2 are shown in Fig. 3. Each panel displays the collected data, grouped into bins 123 arbitrary fluorescence power units wide, by the stippled bars. The statistical uncertainty in the number of counts in each bin is indicated by the error bar. The best-fit fluorescence power distribution given by these data and the theoretical multiple Poisson distribution of Eq. 3 are shown by the heavy solid lines. All fits to Eq. 3

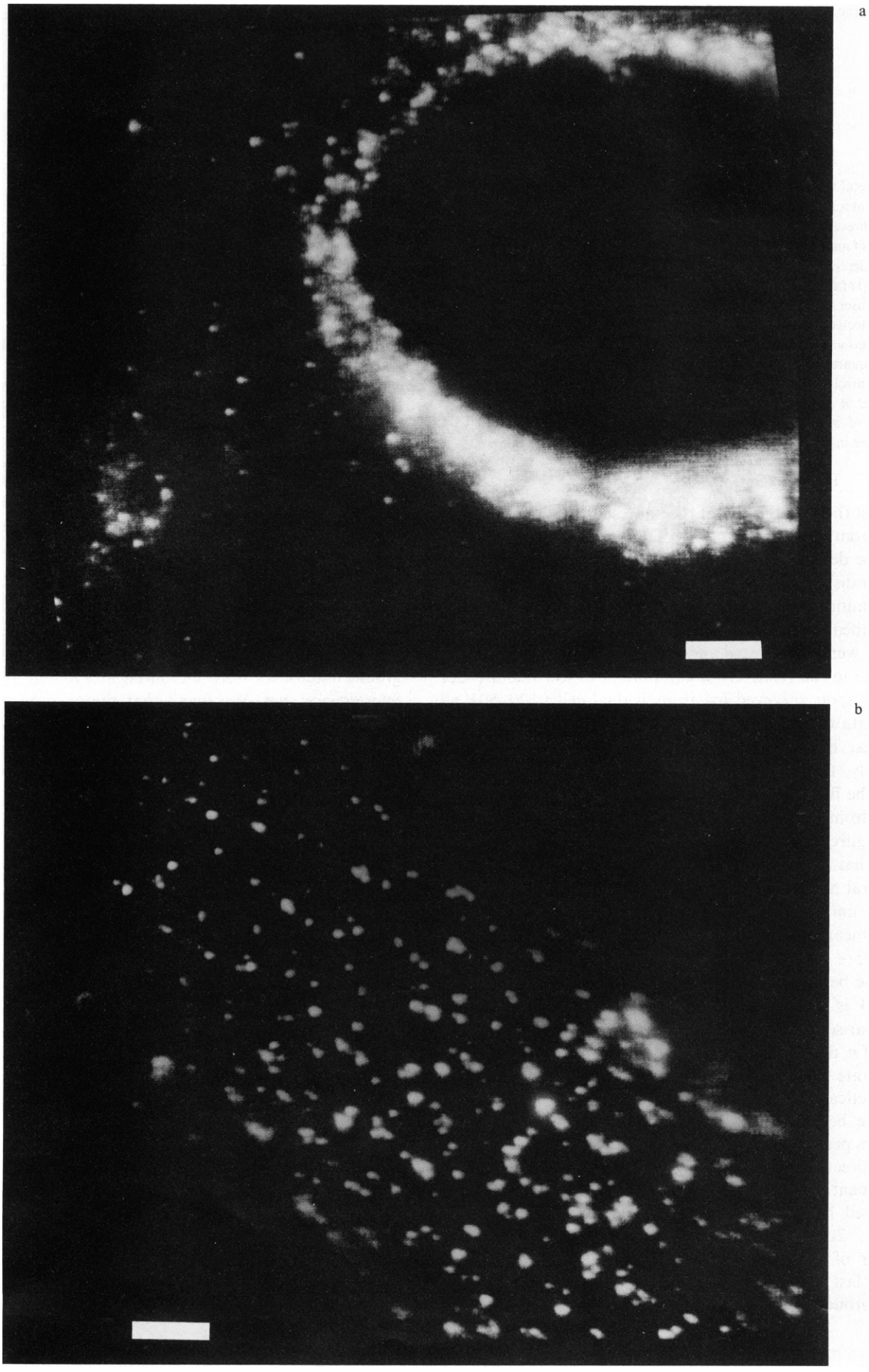

FIGURE 2 Raw fluorescence images of (*a*) an A-431 cell, (*b*) a J.D. (GM2408A) fibroblast, (*c*) a normal (GM3348) fibroblast cell stained at 4°C, and (*d*) a GM3348 fibroblast stained at 22°C. The bars are 5-μm long.

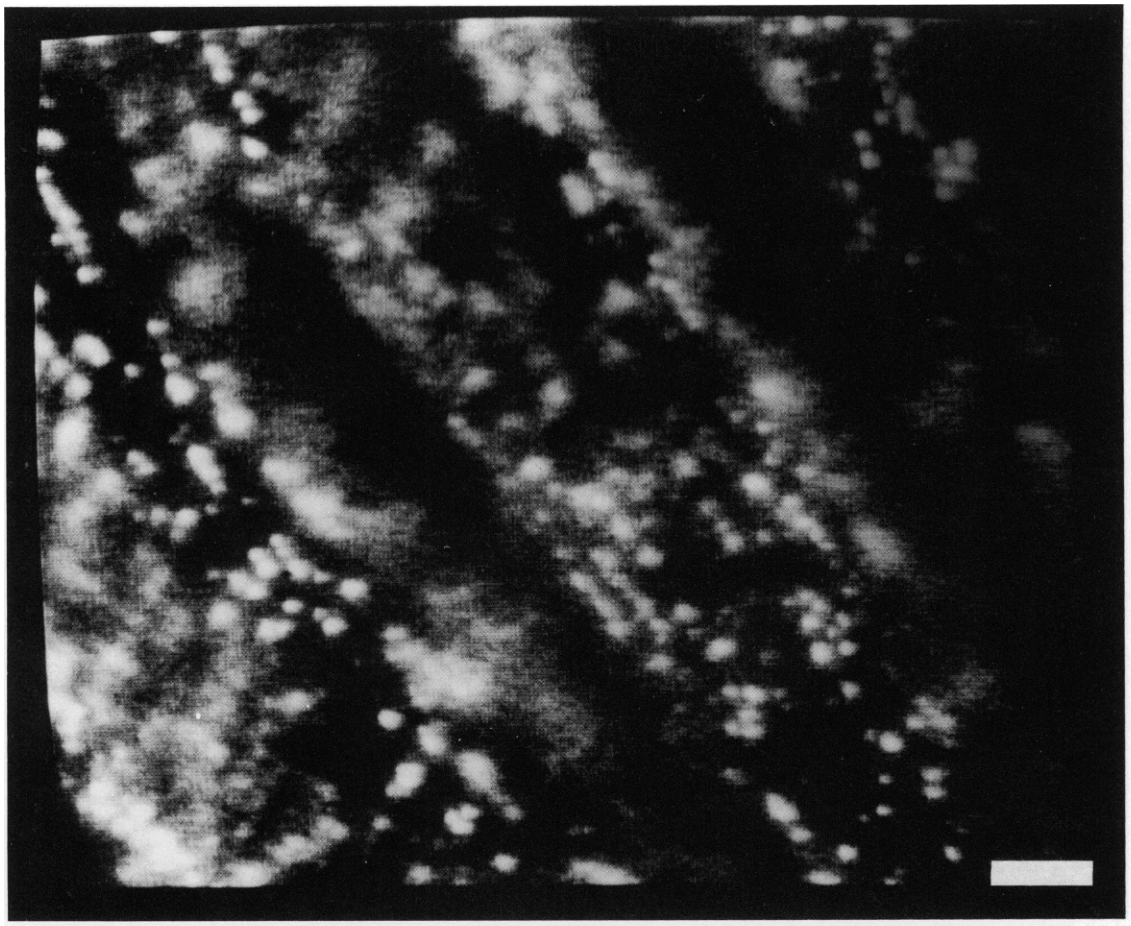

c

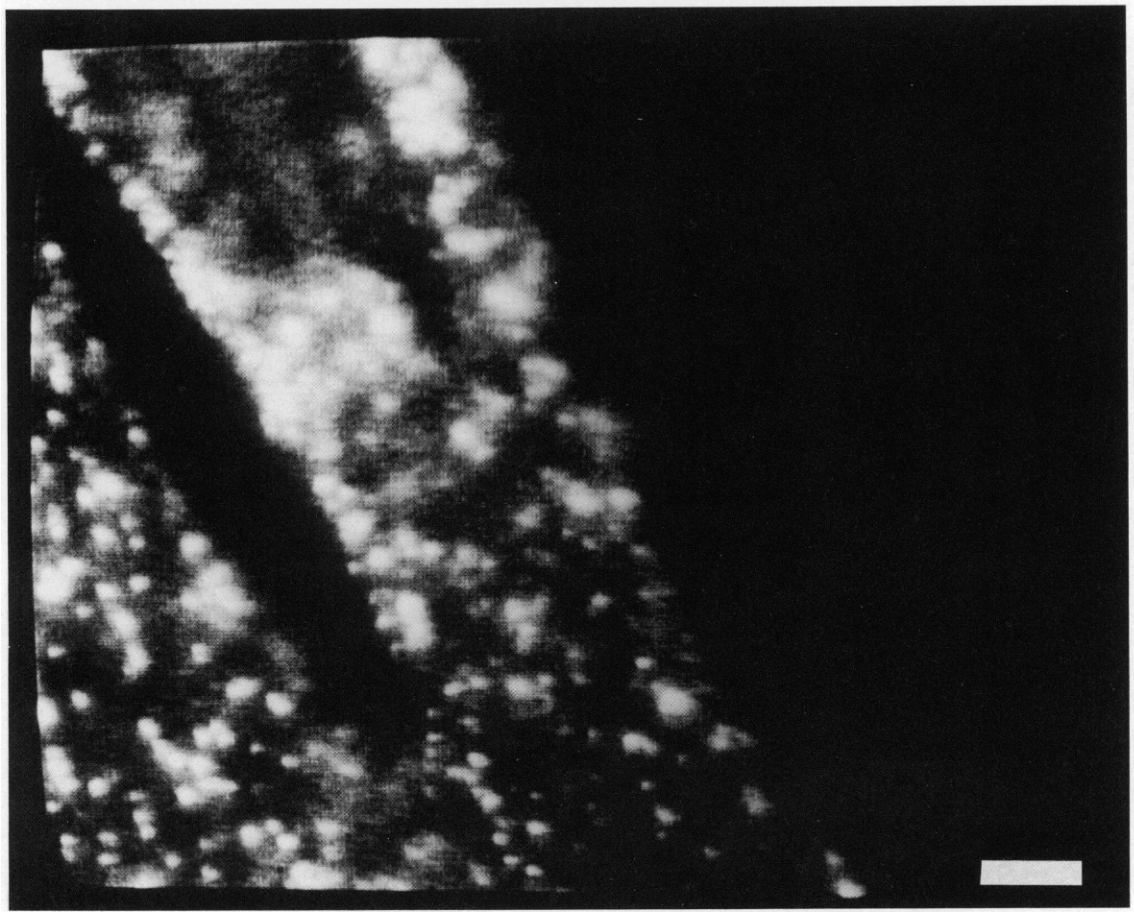

d

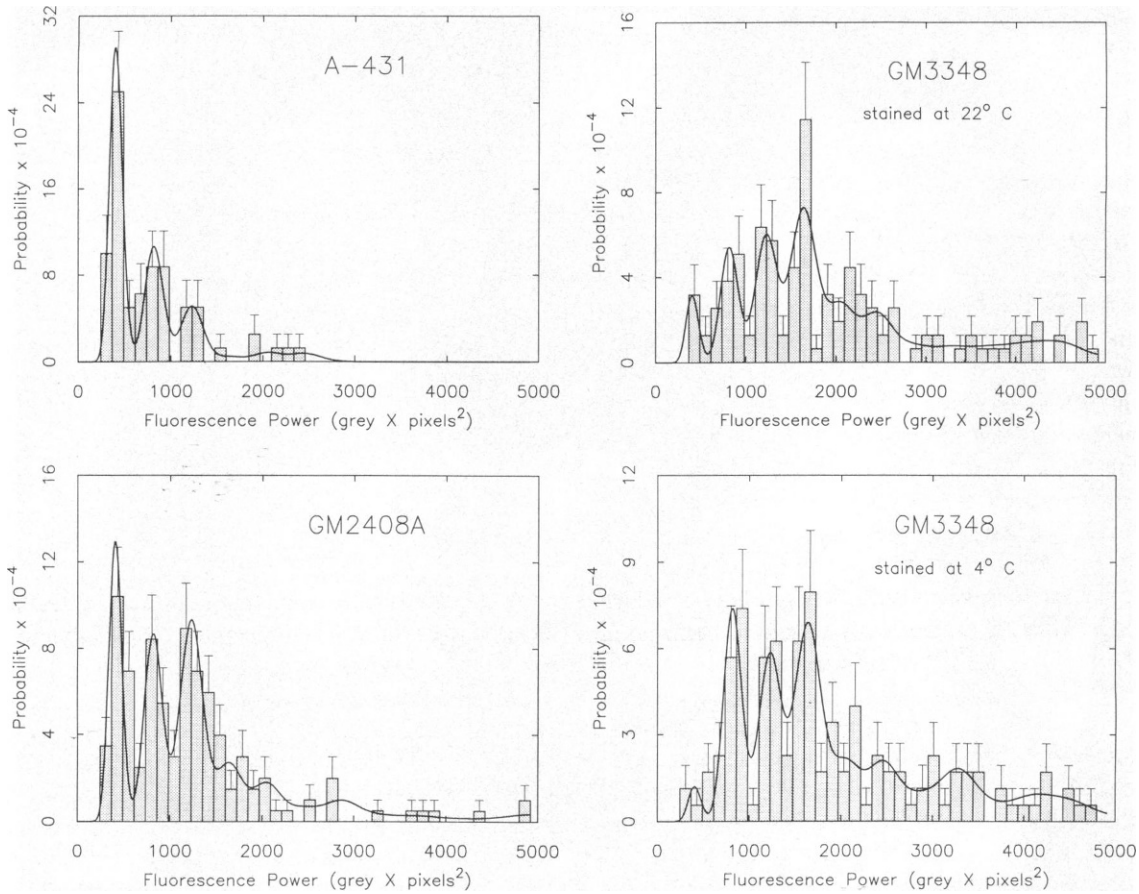

FIGURE 3 Fluorescence power distributions for the cells shown in Fig. 2. (*a*) A-431, (*b*) GM2408A, (*c*) GM3348 stained at 4°C, and (*d*) GM3348 stained at 22°C. The solid curves are the least-squares best fit to Eq. 3 for each data set.

were made with the mean number of fluorophores per dil-LDL held fixed at 35, and the mean intensity of a monomer dil-LDL held fixed at 411 arbitrary fluorescence units, as determined by combining all data as described above. For each distribution, the best-fit analysis was also undertaken for a freely-varying monomer intensity—in all cases the best fit values for that parameter were within 3% (range 403–422) of the nominal value of 411. The tabulated values of the weighting factors for each cluster size in the distributions of Fig. 3 are given in Table I.

From the measured fluorescence power of an individual fluorescence spot in the image of a cell, the number of dil-LDL particles in that spot can now be estimated. To investigate the possibility that regional or global ordering of LDL-RC cluster sizes might be detected on the cell surface, maps of the spatial distribution of cluster sizes of dil-LDL on the above cells were generated. The maps were generated by the digital video system and displayed in color code to assist in the identification of potential long-range ordered structure. The theoretical probability distributions of fluorescence power as calculated from Eq. 2 were used to determine the number of dil-LDL particles represented by the measured power from a given spot. By definition the bounds within which a given amount of

TABLE I
BEST-FIT PROBABILITY DISTRIBUTIONS (IN PERCENT) OF CLUSTERS OF dil-LDL ON THE SURFACES OF HUMAN FIBROBLASTS AND EPIDERMOID CARCINOMA CELLS

Cell type	N_T	Number of dil-LDL particles per cluster												
		1	2	3	4	5	6	7	8	9	10	11	12	13+
A-431	65	51	26	15	2	3	3	0	0	0	0	0	0	0
			92			8			0			0		
GM2408A (J.D.)	165	22	21	28	9	7	2	4	1	1	1	1	2	1
			71			18			6			4		
GM3348 (4°C)	144	2	18	17	24	8	8	3	8	2	4	3	1	1
			37			40			13			8		
GM3348 (22°C)	141	5	12	16	23	9	9	3	3	3	4	4	1	9
			33			41			9			9		

fluorescence power were considered to represent a cluster of size N were delimited by those fluorescence power values at which the $N-1$ and $N+1$ cluster probability distributions were equal to 10% of the N cluster probability distribution. Red dots were generated by the video system at the location of the collected spot fluorescence power values that fell within the $N = 1$ boundary. Likewise, the locations of spot fluorescence power values that fell within other N-mer boundaries were marked by dots of other colors. Any fluorescence values that fell between the N and $N+1$-bounded regions were marked by dots, the right side of which was the color of the N-mer population and the left side of which was the color of the $N+1$-mer population. The regenerated cluster distributions thus produced for the cells of Fig. 2 are shown on the right panels of Fig. 4. Included for reference in Fig. 4 are pseudocolor-enhanced versions of the black and white images of Fig. 2. In this pseudocoloring scheme, the grey scale is broken into eight bands of color, each of which is linearly graded from dark to bright. The effect is dramatically enhanced contrast in the image, particularly for the dimmest of the diI-LDL fluorescence spots.

Examination of Fig. 4 indicates that most of the diI-LDL particles on the surfaces of the A-431 and the GM2408A cells were in clusters of from 1 to 3 particles, and that the spatial distribution of these clusters is apparently random. The distribution of clusters on the normal fibroblast line GM3348, which was stained at 4°C shows that larger clusters of diI-LDL are aligned in quasilinear arrays, a pattern that has been reported for coated pits on human fibroblasts (5). The much less numerous population of small clusters on this cell type is randomly arranged. For the normal fibroblasts that were stained at 22°C, the spatial arrangement of diI-LDL clusters is much the same as for the normal fibroblast stained at 4°C, although a subpopulation of very large clusters is now found (Table I). This result is shown graphically in Fig. 5, where the normalized number of clusters is plotted vs. cluster size for the cells of Fig. 1. Note the appearance of clusters of size ~20 for the normal fibroblast stained at 22°C.

DISCUSSION

The data and analysis presented here demonstrate that it is possible to measure the spatial distribution of diI-LDL clusters on individual cells by the techniques of digital video microscopy and image processing. Further, it is demonstrated that the number of diI-LDL particles in a given location can be counted by this optical technique and that the distribution of numbers of LDL particles per cluster can be reliably compared from individual cell to cell.

The clustering detected in these experiments reflects only that clustering of the ligand-receptor complex after ligand challenge. Pitas et al. and Innerarity et al. (17, 18) have shown that LDL, which contains the receptor-binding protein apo-B, binds to a single site on the surface of human cells in contrast with apo-E containing HDL_c, which binds four of the single apo-B,E binding sites. Pitas et al. (19) have further shown that the receptor sites that bind a single LDL particle can bind up to two apo-E dimyristoyl-phosphatidylcholine vesicles. This dual apo-E DMPC vesicle binding is presumably due to a lack of steric hindrance of the vesicles, which is present for LDL and HDL_c.

The use of a fluorescent probe, such as diI-LDL, to monitor in the optical microscope the spatial distribution and clustering of individual LDL-receptor complexes on the cell surface has two important advantages over electron microscope counting of electron-dense labels attached to LDL or its receptor. First, the ease of use of the fluorescent label and the retention of morphological structure with this technique allows one to prepare rapidly and measure the fluorescence associated with a set of cells that have not been subjected to harsh fixation, dehydration, and embedding procedures. Second, this fluorescence technique can be used to examine LDL-receptor complex dynamics as the technique can be applied to living cells. Of course a disadvantage of this technique relative to electron microscopy imaging is its lower spatial resolution.

We have shown that the distribution of LDL-RC on the surfaces of A-431 human epidermoid carcinoma cells and of human mutant GM2408A (J.D.) fibroblasts is weighted heavily toward the cluster sizes of 1–3, which is consistent with the notion that both of these cell lines express LDL receptors with defective clathrin-coated pit binding (10, 13) since the receptors would not cluster in the coated pits. Anderson et al. (13) describe LDL-ferritin particles on A-431 cells as being in large clusters containing up to 35 ferritin particles per cluster, particularly on surface extensions, and in smaller clusters of seven ferritin particles contained in coated pits. As the LDL-ferritin complex employed in the study contained from 1 to 3 ferritin particles per LDL (20), the largest clusters on A-431 as measured by Anderson et al. number up to ~17 LDL particles, while coated pits contain ~4 LDL particles. The uncertainty in these values is quite high if one assumes that the bonding of ferritin to LDL follows the same Poisson distribution of Eq. 1, since the spread of the distribution is quite high when the mean number n of ferritin cores per LDL is of the order of 2. This broadening effect of small n smears together the probability for even the 1 and 2 particle cluster distribution functions as seen from Eq. 2. Thus, our results are consistent with those of Anderson et al. within measurement uncertainties.

To count accurately the number of particles tagged by n labels, fluorescent or electron-dense, n should be large or exactly an integer. The first case is satisfied by diI-LDL for which n is ~40. The second case could be satisfied by a carefully prepared probe-ligand conjugate (as for monomeric insulin-ferritin [21]) or by a phycobiliprotein, which is sufficiently fluorescent to be visualized and yet contains unitary fluorescence (22).

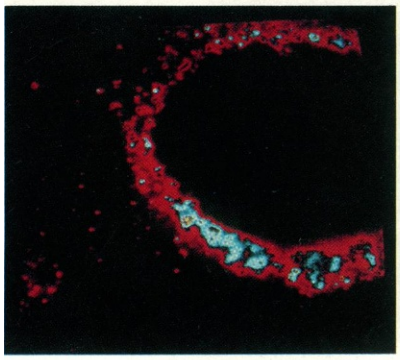


A-431
1
2
3
4
5
6
7+

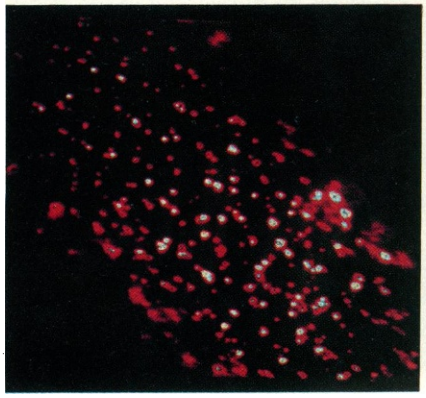


GM2408A
1
2
3
4
5
6
7+

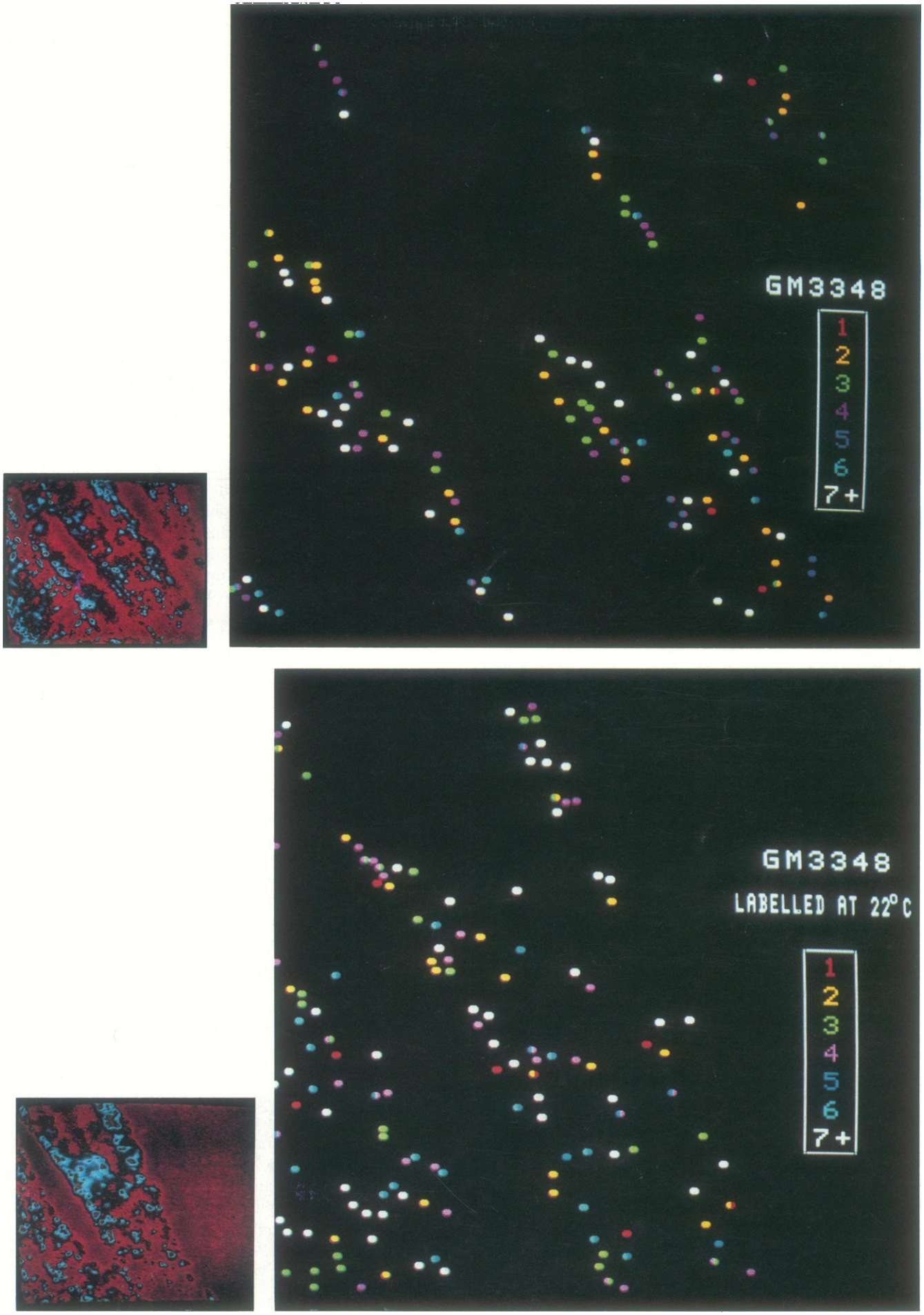

FIGURE 4 Pseudocolor fluorescence images (*a–d*) and reconstructed cluster size spatial distributions (*e–h*) for A-431 (*a, e*), GM2408A cells (*b, f*), GM3348 cells stained at 4°C (*c, g*), and GM3348 cells stained at 22°C (*d, h*) for the same cells shown in Fig. 2. Note the random distributions of clusters of various sizes except for the linear arrays on the normal (GM3348) cells.

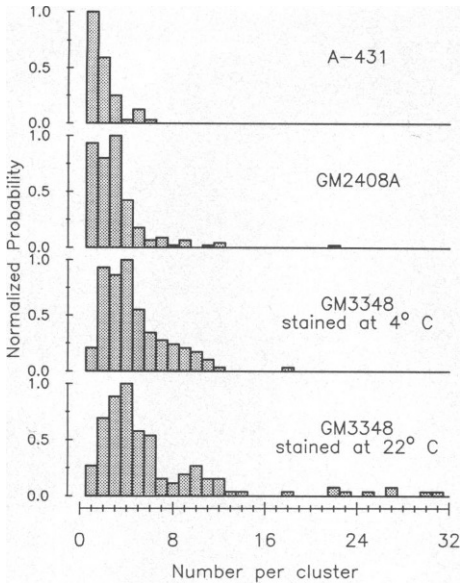

FIGURE 5 The normalized probability distributions of numbers of diI-LDL particles as measured on the four cells of Fig. 2. Note the appearance of large-size (19-32) diI-LDL clusters on the normal GM3348 cell stained at 22°C (*bottom distribution*).

Although we did not observe the very large cluster sizes described by Anderson et al., our measurements were confined to the flat lamellipodium of the cell in Fig. 2*a*. One should note that the area of the cell that is out of focus contains a large number of diI-LDL particles as judged by the fluorescence intensity emanating from it; this region may well contain cluster sizes different from what were detected on the flat lamellipodium, and that could correspond to the large size clusters on cell surface extensions as noted above.

The clustering of diI-LDL particles on normal human fibroblasts indicates that a significant population, which is grouped together in unresolved clusters containing four or more LDL-RC (Table I) exists, while there is a smaller population of particles in clusters of from 1 to 3. We think this indicates that the larger size clusters, which are much less predominant on GM2408A fibroblasts or A-431 carcinoma cells, are those clusters of liganded LDL receptors in coated pits, as the receptors on these cells are known to precluster in these regions (20, 23). Anderson et al. found four to six ferritin particles per coated pit in normal cells translating to an average of two to three LDL particles per pit (20). As the counting of LDL-ferritin particles was done on thin sections of cell membrane in both this study and the one on A-431 cells, one might suspect that the mean number of LDL particles per coated pit was underestimated by a factor of the ratio of the thickness of the section to the dimension of a coated pit, since only a portion of the coated pit was sampled by the sectioning process. Thus, it is difficult to compare directly the results described in this paper and those of Anderson et al.

The subpopulation of diI-LDL particles on normal cells detected as individuals or clusters of size 2-3 may well represent LDL-Rs that were expressed on the cell surface just before or during ligand challenge and LDL-Rs that did not have sufficient time to move to coated pits. This assumption is supported by the fact that clusters of the size 1-3 are predominant in the cluster distributions of GM2408A and A-431 cells, for which it is known that LDL-RCs do not readily associate with coated pits on the cell surface. Our results are similar to those described by Goldstein et al., in which they note that about two-thirds of the LDL-RC on normal cells are in coated pits while one-third of the LDL-RC are diffusely distributed on the uncoated regions of the cell surface (1).

The population of diI-LDL clusters found near the plasma membrane of normal GM3348 fibroblasts stained at room temperature rather than at 4°C shows a dramatic change in the distribution of cluster size as shown in Fig. 5 and Table I. Single, unresolved clusters from 19 to 32 diI-LDL particles per cluster appear in the distribution, while no such large clusters were found on the chilled cells, a result that has recently been confirmed on several more GM3348 fibroblasts (R. Ghosh and W. W. Webb, unpublished observation). We attribute these large collections of diI-LDL to the first stages of the endocytosis process, which is known to proceed at rates consistent with the time course of ~15 min at 22°C (2). As the large clusters we observe are very near the plasma membrane (see Fig . 2 and note that the depth of focus of the 100× objective used was ~0.25 μm), these large clusters may be LDL-containing coated endocytic vesicles that have just coalesced or fused preparatory to entry into the cytoplasmic transport machinery for distribution to the sites of ligand-receptor uncoupling and ligand degradation. It is quite feasible to examine this process using our technique along with anti-clathrin immunofluorescence staining to monitor the relative disposition of LDL as a function of time in a living cell. This early time processing in endocytosis is a topic of current interest (2, 24, 25).

An early result of Anderson et al. (26) indicated that a transient increase in the number of ferritin-LDL particles in coated pits on normal cells increased by about threefold after four min of incubation at 37°C. It is interesting to note that we find a population of clusters of LDL with a threefold to fourfold larger size than the median of the population for nonincubated cells as seen in Fig. 5. Thus, the clusters of 19-32 LDL-RC that we detect on cells stained at 22°C may also be coated-pit associated clusters that formed after ligand challenge. Again, the application of our techniques to living cells can elucidate this process.

The use of quantitative fluorescence imaging in combination with a well-characterized probe such as diI-LDL has proven to be a powerful probe of cell membrane morphology and dynamics. The technique we have described here has applications to many aspects of cell function, particularly to the mechanism of endocytosis and receptor trafficking, both on the cell surface and in the

cytoplasm. We are presently applying this technique to the time dynamics of LDL-RC surface mobility and intracellular vesicular transport.

This work was supported by grants from the National Science Foundation grant PCM-83-03404 , National Institute of Health grant GM33028-02, and the Cornell Biotechnology Program.

REFERENCES

1. Goldstein, J. L., R. G. W. Anderson, and M. S. Brown. 1979. Coated pits, coated vesicles, and receptor-mediated endocytosis. *Nature (Lond.).* 279:679–685.
2. Pastan, I. H., and M. C. Willingham. 1981. Receptor-mediated endocytosis of hormones in cultured cells. *Annu. Rev. Physiol.* 43:239–250.
3. Schlessinger, J., Y. Schecter, P. Curecasas, M. C. Willingham, and I. Pastan. 1978. Quantitative determination of the lateral diffusion coefficients of the hormone-receptor complexes of insulin and epidermal growth factor on the plasma membrane of cultured human fibroblasts. *Proc. Natl. Acad. Sci. USA.* 75:5353–5357.
4. Schlessinger, J., Y. Schecter, M. C. Willingham, and I. Pastan. 1978. Direct visualization of the binding, aggregation, and internalization of insulin and epidermal growth factor of fibroblastic cells. *Proc. Natl. Acad. Sci. USA.* 75:2135–2139.
5. Anderson, R. G. W., E. Visile, R. J. Mello, M. S. Brown, and J. L. Goldstein. 1978. Immunocytochemical visualization of coated pits and vesicles in human fibroblasts: relation to low density lipoprotein receptor distribution. *Cell.* 15:919–933.
6. Brown, M. S., and J. L. Goldstein. 1979. Receptor-mediated endocytosis: Insights from the lipoprotein receptor system. *Proc. Natl. Acad. Sci. USA.* 76:3330–3337.
7. Yamamoto, T., C. G. Davis, M. S. Brown, W. J. Schneider, M. L. Casey, J. L. Goldstein, and D. W. Russell. 1984. The human LDL receptor: A cysteine-rich protein with multiple Alu sequences in its mRNA. *Cell.* 39:27–38.
8. Russell, D. W., W. J. Schneider, T. Yamamoto, K. L. Luskey, M. S. Brown, and J. L. Goldstein. 1984. Domain map of the LDL receptor: Sequence homology with the epidermal growth factor precursor. *Cell.* 37:5 77–585.
9. Südhof, T. C., J. L. Goldstein, M. S. Brown, and D. W. Russell. 1985. The LDL receptor gene: A mosaic of exons shared with different proteins. *Science (Wash. DC).* 228:815–822.
10. Brown, M. S., and J. L. Goldstein. 1976. Analysis of a mutant strain of human fibroblasts with a defect in the internalization of receptor-bound low density lipoprotein. *Cell.* 10:663–674.
11. Goldstein, J. L., and M. S. Brown. 1977. Genetics of the LDL receptor: Evidence that the mutations affecting binding and internalization are allelic. *Cell.* 12:692–641.
12. Barak, L. S., and W. W. Webb. 1982. Diffusion of low density lipoprotein-receptor complex on human fibroblasts. *J. Cell Biol.* 95:846–852.
13. Anderson, R. G. W., M. S. Brown, and J. Goldstein. 1981. Inefficient internalization of receptor-bound low density lipoprotein in human carcinoma A-431 cells. *J. Cell Biol.* 88:441–452.
14. Staples, R. C., D. Gross, R. Tiburzy, H. C. Hoch, S. Hassouna, and W. W. Webb. 1984. Changes in DNA content of nuclei in rust uredospore germlings during the start of differentiation. *Exp. Mycol.* 8:245–255.
15. Brown, M. S., S. E. Dana, and J. L. Goldstein. 1974. Regulation of 3-hydroxy-3-methyl-glutaryl coenzyme A reductase activity in cultured human fibroblasts. *J. Biol. Chem.* 249:789–796.
16. Barak, L. S., and W. W. Webb. 1981. Fluorescent low density lipoprotein for observation of dynamics of individual receptor complexes on cultured human fibroblasts. *J. Cell Biol.* 90:595–604.
17. Pitas, R. E., T. L. Innerarity, K. S. Arnold, and R. W. Mahley. 1979. Rate and equilibrium constants for binding of apo-E HDL_c (a cholesterol-induced lipoprotein) and low density liproteins to human fibroblasts: evidence for multiple receptor binding of apo-E HDL_c. *Proc. Natl. Acad. Sci. USA.* 76:2311–2315.
18. Innerarity, T. L., R. E. Pitas, and R. W. Mahley. 1980. Receptor binding of cholesterol-induced high-density lipoproteins containing predominantly apoprotein E to cultured fibroblasts with mutations at the low-density lipoprotein receptor locus. *Biochemistry.* 19:4359–4365.
19. Pitas, R. E., T. L. Innerarity, and R. W. Mahley. 1980. Cell surface receptor binding of phospholipid · protein complexes containing different ratios of receptor-active and -inactive E apoprotein. *J. Biol. Chem.* 255:5454–5460.
20. Anderson, R. G. W., J. L. Goldstein, and M. S. Brown. 1976. Localization of low density lipoprotein receptors on plasma membranes of normal human fibroblasts and their absence in cells from a familial hypercholesterolemia homozygote. *Sci. USA.* 73:2434–2438.
21. Jarett, L., and R. M. Smith. 1983. Partial disruption of naturally-occurring groups of insulin receptors on adipocyte plasma membranes by dithiothreitol and *N*-ethylmaleimide: The role of disulfide bonds. *Proc. Natl. Acad. Sci. USA.* 80:1023–1027.
22. Oi, V. T., A. N. Glaser, and L. Stryer. 1982. Fluorescent phycobiliprotein conjugates for analysis of cells and molecules. *J. Cell Biol.* 93:981–986.
23. Carpentier, J.-L., P. Gorden, J. L. Goldstein, R. G. W. Anderson, M. S. Brown, and L. Orci. 1979. Binding and internalization of ^{125}I-LDL in normal and mutant human fibroblasts: a quantitative autoradiographic study. *Exp. Cell Res.* 121:135–142.
24. Willingham, M. C., and I. Pastan. 1983. Formation of receptosomes from plasma membrane coated pits during endocytosis: analysis by serial sections with improved membrane labeling and preservation techniques. *Proc. Natl. Acad. Sci. USA.* 80:5617–5621.
25. Geuze, H. J., J. W. Slot, G. J. A. M. Strous, H. F. Lodish, and A. L. Schwartz. 1983. Intracellular site of asiloglycoprotein receptor-ligand uncoupling: double-label immunoelectron microscopy during receptor-mediated endocytosis. *Cell.* 32:277–287.
26. Anderson, R. G. W., M. S. Brown, and J. L. Goldstein. 1977. Role of the coated endocytic vesicle in the uptake of receptor-bound low density lipoprotein in human fibroblasts. *Cell.* 10:351-364.